Research Report

2014-07

Comparative Study on Novel Dual Stator Radial Flux and Axial Flux Permanent Magnet Motors with Ferrite Magnets for Traction Application

W. Zhao, T. A. Lipo*, B. Kwon

Department of Electronic Systems Engineering
Hanyang University
Ansan, 426-791, Korea

*Department of Electrical and Computer Engineering
University of Wisconsin-Madison
Madison, WI 53706 USA

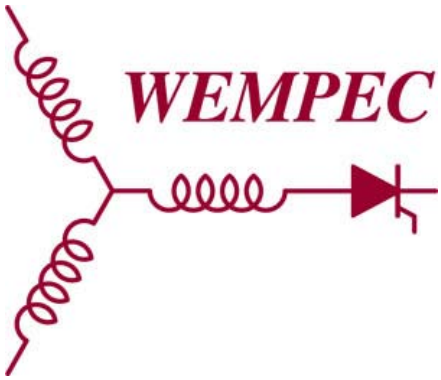

Wisconsin
Electric
Machines &
Power
Electronics
Consortium

University of Wisconsin-Madison
College of Engineering
Wisconsin Power Electronics Research Center
2559D Engineering Hall
1415 Engineering Drive
Madison WI 53706-1691

Comparative Study on Novel Dual Stator Radial Flux and Axial Flux Permanent Magnet Motors with Ferrite Magnets for Traction Application

Wenliang Zhao[1], Thomas A. Lipo[2], *Life Fellow, IEEE*, and Byung-Il Kwon[1], *Senior Member, IEEE*

[1]Department of Electronic Systems Engineering, Hanyang University, Ansan, 426-791, Korea
[2]Department of Electrical and Computer Engineering, University of Wisconsin-Madison, Madison, WI 53706 USA

High performance synchronous motors with less or no rare earth magnets for hybrid electric vehicles (HEVs) have attracted much attention due to the high cost and limited supply of the rare earth materials. Accordingly, this paper proposes two novel traction motors with ferrite magnets for HEVs, which have competitive torque density and efficiency as well as operation range with respect to a referenced rare earth magnet motor employed in the third-generation Toyota Prius, a commercialized HEV. The two proposed traction motors named as dual stator radial flux permanent magnet motor (DSRFPMM) and dual stator axial flux permanent magnet motor (DSAFPMM) adopt the same design concept which incorporate the unaligned arrangement of two stators together with the use of spoke-type magnet array and phase-group concentrated-coil winding for the purpose of increasing torque density and reducing torque ripple. Finite element method (FEM) is utilized for predicting the main characteristics such as back EMF, cogging torque, electromagnetic torque, iron loss and efficiency in both motors. Moreover, a comparative study between the proposed DSRFPMM and DSRFPMM is performed under the same rated power condition. As a result, it is demonstrated that both the proposed ferrite permanent magnet motors could be good alternatives for traction application replacing the rare earth magnet motors.

***Index Terms*—Axial flux permanent magnet motor (AFPMM), dual stator, finite element method (FEM), ferrite permanent magnet motors, hybrid electric vehicles (HEVs), radial flux permanent magnet motor (RFPMM), traction motors, torque density.**

I. Introduction

Recently, a demand for developing electrical propulsion systems with high torque density, high efficiency and low cost for hybrid electric vehicles (HEVs) are becoming more and more attractive due to the environment and energy consideration. In order to satisfy the demand, permanent magnet synchronous motors (PMSMs) with rare earth magnets have been mostly employed as the main traction motors benefitting from the excellent properties of rare earth magnets. However, the rare earth materials such as Neodymium and Dysprosium in rare earth magnets exhibit the problem of high cost and limited supply, which brings a serious challenge for the mass production of HEVs. Therefore, continuation of research for development of high performance synchronous motors with less or no rare earth magnets is of importance.

Accordingly, several substitute motors with reduced or free of rare earth magnets have been investigated [1]-[5]. Compared with induction motors and switched reluctance motors, PMSMs with ferrite magnets are thought to be better candidates considering their efficiency and vibration properties, and especially, their feature of making possible use of both reaction torque and reluctance torque. However, conventional ferrite magnet motors generally have much poorer torque/power density than rare earth magnet motors due to the lesser properties of ferrite PMs. Although some ferrite PM motors adopting novel techniques such as a segmented rotor structure have been proposed for improving torque/power density [5], a gap still exists to achieve the target performance required to replace rare earth PM motors under the same operation condition. In [6], a novel structure for axial flux PM motor incorporating the unaligned arrangement of two stators together with the use of spoke-type permanent magnet array and phase-group concentrated-coil winding was explored for the purpose of increasing torque density and reducing torque ripple. In this paper, the idea is extended to radial flux PM motors and a comparative study is performed between a dual stator radial flux permanent magnet motor (DSRFPMM) and a dual stator axial flux permanent magnet motor (DSAFPMM).

The proposed two motors are designed as traction motors using ferrite permanent magnets competitive to the target values from the rare earth magnet motor mounted in the third-generation Toyota Prius, a commercialized HEV. The investigation of motor performance is based on the same outer diameter and axial length as well as the same operation ratings such as rate speed and rated power as those of the referenced rare earth magnet motor. The main characteristics such as back EMF, cogging torque, electromagnetic torque, iron loss and efficiency of both proposed motors are predicted by the finite element method (FEM).

II. Motor Topologies and Operation Principle

A. Basic Design Rules

Based on the design concept as shown in Fig. 1, a specific combination of stator slots and magnet poles depending on the phase group concentrated-coil winding construction was deduced as expressed in [6]. The number of slots in one stator for three phases is

$$Q = 3\, n_1 n_2 \quad (1)$$

The number of magnet poles is

$$2p = 3\, n_1 n_2 + n_2 \quad (2)$$

where n_1 is defined as the number of coils for one phase group, n_2 is the number of groups for one phase. It is noted here the slot and teeth width within one phase group are designed to be

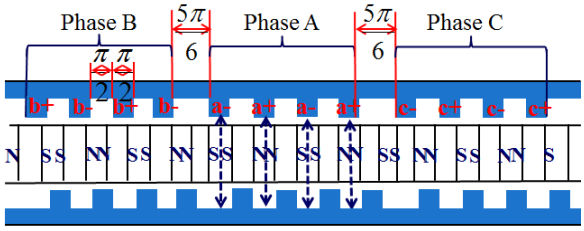

Fig. 1. Design concept.

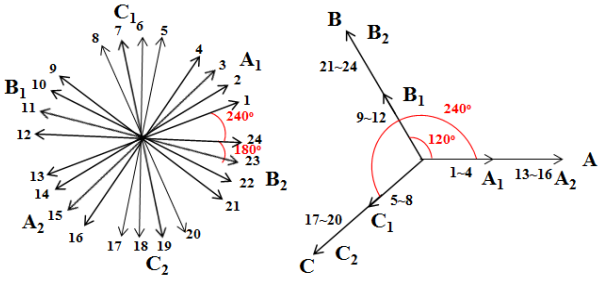

Fig. 2. Winding configuration and resultant EMF vector.

$\pi/2$ (elec.), while the slot width between two different phases is $5\pi/6$ (elec.) for producing 3-phase balanced back EMF. Assuming that the combination of n_1=4 and n_2=2 is selected, the resultant EMF vector is shown in Fig. 2. Due to the opposite polarity of adjacent coils and the alternate magnetization directions in permanent magnets, the induced EMF of every coil will follow the same direction resulting in the largest EMF vector.

B. Motor Topologies

The proposed DSRFPMM and DSAFPMM are shown in Fig. 3. Their specifications with respect to the target values are illustrated in Table I. Both motors feature the same outer diameter and axial length as the target motor as well as considering the dimension of winding end turns. Ferrite magnets are circumferentially magnetized with alternately reversed magnetization direction in polarity and arranged as spoke-type array for air gap flux magnification. Phase-group concentrated-coil stator windings are wound around each stator tooth and the two stators adopt axially unaligned configuration displaced by one tooth width. The target maximum torque and power are 207 Nm and 60 kW or greater at the rated speed of 2768 rpm, thus, the torque and power density are above 35Nm/L and 10.2kW/L, respectively. The efficiency will be kept above 91%, while the current density is designed to be below 19 A/mm^2 assuming liquid cooling.

C. Operation Principle

The operation principle of two designed traction motors is illustrated in Fig. 4. Within one phase group, when the rotor pole rotates to become aligned with the teeth of upper stator and the slot of lower stator, almost the total PM flux will flow through the upper airgap, reaching the maximum of flux as the case 1. Similarly, the same effects will occur in the lower airgap of case 2. Assuming that sinusoidal currents are injected into the coils, a higher resultant torque can be obtained than conventional motors in which two air gaps work independently, while this fact has been verified in [6].

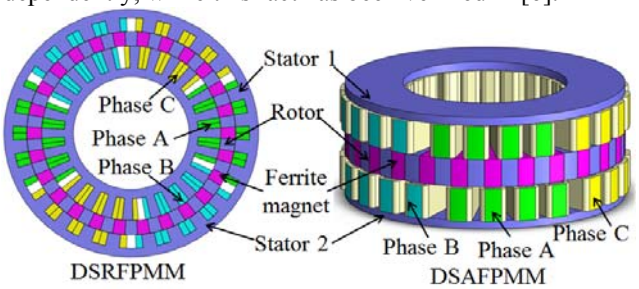

Fig. 3. Topologies of DSRFPMM and DSAFPMM.

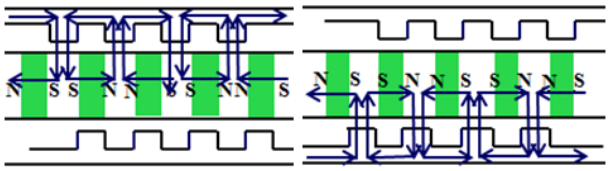

<case 1> <case 2>

Fig. 4. Operating principle.

TABLE I
Specifications of Designed DSRFPMM and DSAFPMM

Item	Unit	Target	DSRFPMM	DSAFPMM
Magnets	-	NdFeB	Ferrite/0.43T	
Outer diameter of motor	mm	264	264	255 End turn:9
Axial length of motor	mm	108	95 End turn:13	108
Airgap	mm	-	0.9 / 1.0	1.2*2
Max. torque	Nm	207	≥ 207	
Max. output power	kW	60	≥ 60	
Current density	A/mm^2	19	≤ 19	
Efficiency@2768rpm	%	91	≥ 91	
Max. power density	kW/L	10.2	≥ 10.2	
Max. torque density	Nm/L	35	≥ 35	

III. FEA Results and Discussion

A. Magnetic Flux Density, Back EMF and Cogging Torque

The magnetic flux density distribution was carried out at the rated speed condition. The no load case displaying the position of maximum flux for phase A in outer/upper stator winding is shown in Fig. 5(a). As is stated in the operation principle, almost total PM flux of the proposed motors flows into the outer/upper air gap corresponding to phase A of outer/upper stator winding, thus leading to higher airgap flux density than

the conventional motors in which two air gaps work independently. The magnetic flux density distribution at full load condition is shown in Fig. 5(b). The magnetic flux density in the iron core is below 1.8 T despite that slight saturation is occurred in the edge of stator teeth and rotor pole.

The 3-phase balanced back EMF aiming at verifying the stator design concept is shown in Fig. 6. Fig. 7 demonstrates the advantage of unaligned arrangement of two stators in cogging torque minimization. The peak to peak values of cogging torque in the proposed DSRFPMM and DSAFPMM are 1.826 Nm and 1.135 Nm, respectively, which are 0.9 % and 0.5 % with respect to their rated torque. The DSRFPMM contains higher cogging torque than the DSAFPMM due to the adoption of a smaller air gap.

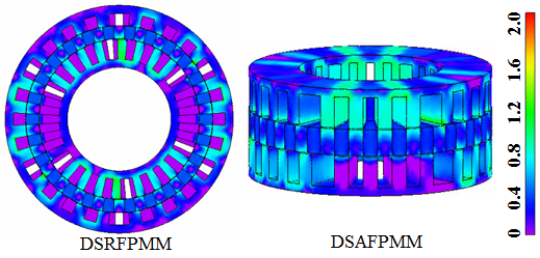

(a) Magnetic flux density without load

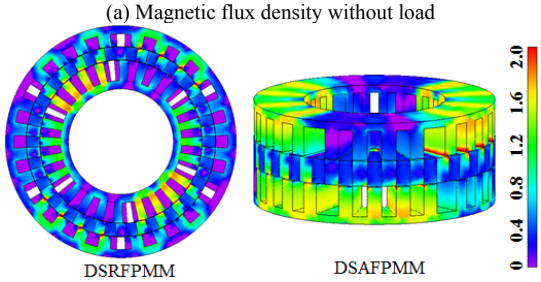

(b) Magnetic flux density with full load

Fig. 5. Magnetic flux density distribution.

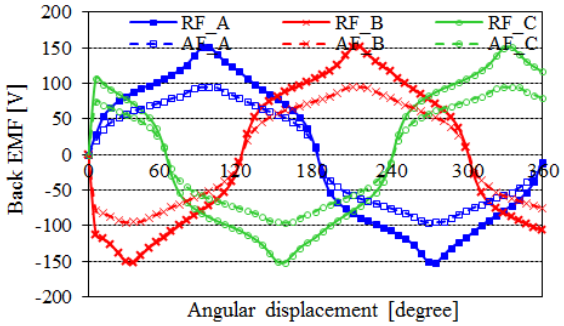

Fig. 6. Three phase back EMF.

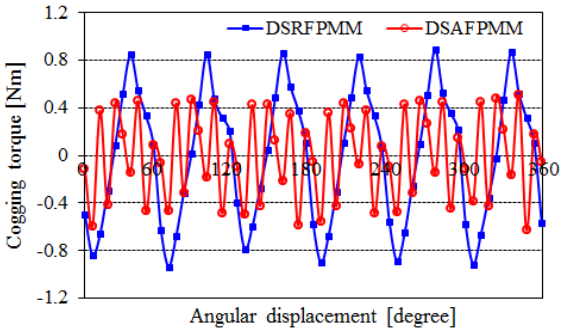

Fig. 7. Cogging torque.

B. Torque Characteristics

The electromagnetic torque for both proposed motors is obtained by feeding with a three phase balanced sinusoidal current source for the sake of performance estimation. Fig. 8 shows the relationship between the average torque and current phase angle. The maximum average torque for the DSRFPMM and DSAFPMM is the same as 208.8 Nm at the current phase angle of 20 degree and 15 degree, respectively. Thus, the maximum torque for both motors is 60.5 kW which slightly exceeds the target vale. The instantaneous torque with respect to the rotational angle for both proposed motors is shown in Fig. 9. The torque ripple ratio defined as the difference of peak to peak torque value to average torque value for the DSAFPMM is 5.5 %, while it is 10.0% for the DSRFPMM resulting from the smaller airgap.

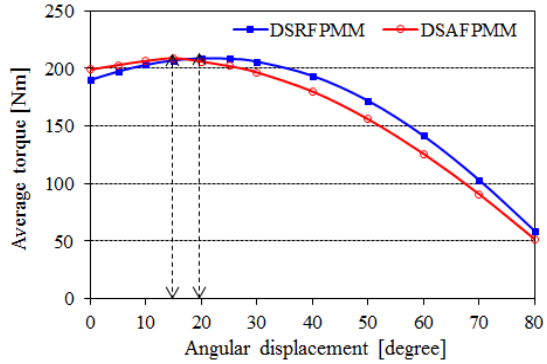

Fig. 8. Average torque with respect to current phase angle.

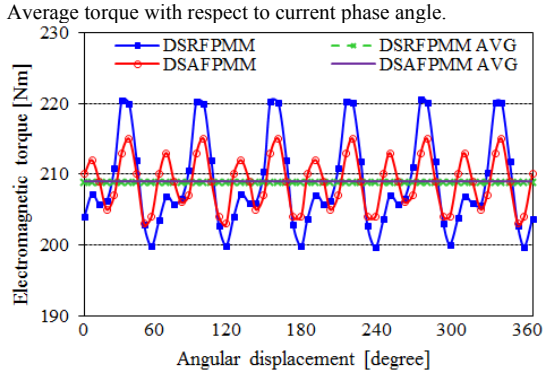

Fig. 9. Electromagnetic torque with respect to rotational angle.

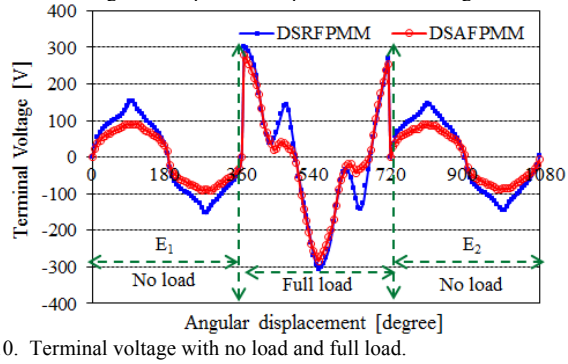

Fig. 10. Terminal voltage with no load and full load.

The volumetric torque/power density of both proposed motors are the same value of 35.33 Nm/L, while the DSAFPMM has higher torque/power-weight ratio than the DSRFPMM due to the less usage of magnets and iron core. The results of performance estimation by FEM are summarized in Table II.

C. Demagnetization Analysis

The irreversible demagnetization of the ferrite magnets in both proposed motors is evaluated at the rated current of 18 Arms/mm^2 under rated speed condition. The demagnetizing ratio is defined as:

$$\delta = \frac{E_1 - E_2}{E_1} \tag{3}$$

where E_1 is the rms value of the terminal voltage in phase before feeding with current excitation, and E_2 is the rms value of the terminal voltage in phase after feeding with current excitation as shown in Fig.10. The demagnetization ratio for the DSRFPMM is 3.0%, while it is 3.2% for the DSAFPMM, which demonstrates that both proposed motors have good endurance against the irreversible demagnetization despite that only a slight demagnetization is occurred in the edge of the ferrite magnets.

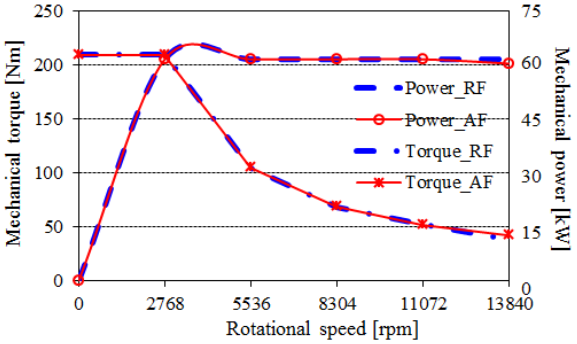

Fig. 11. Constant torque and constant power region with FW control.

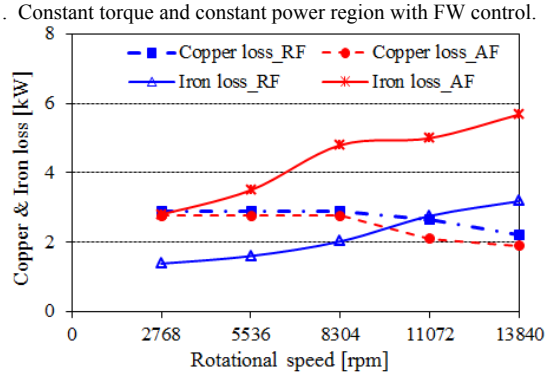

Fig. 12. Copper loss and iron loss over the constant power region.

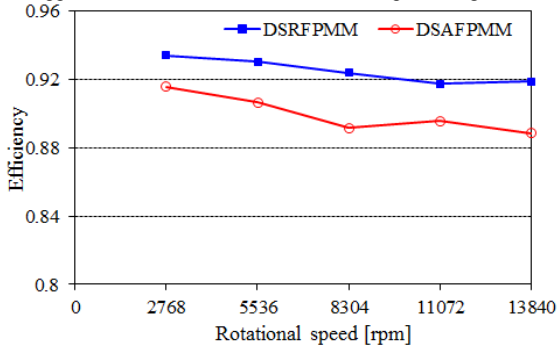

Fig. 13. Efficiency during the constant power region.

D. Operation Range, Loss and Efficiency

Fig. 11 shows the simulated characteristics in the constant torque and constant power region with the flux weakening control strategy. The results demonstrate that both proposed motors have the capability of producing 60 kW of mechanical power over a 5:1 speed range. The loss and efficiency are investigated under constant power load as shown in Fig. 12 and Fig. 13, respectively. The copper loss is determined by

$$P_{copper} = 3I_{rms}^2 R \tag{4}$$

where I_{rms} is the rms value of armature current, and R is the stator resistance.

The iron loss is estimated by FEM modeling employing the commercial software JMAG which is based on the equation

$$P_{iron} = \sum_{i}^{N_{element}} [P_{h_i}(B, f_e) + P_{e_i}(B, f_e)] \tag{5}$$

where $N_{element}$ is the element number, $P_{hi}(B,fe)$ is the hysteresis loss of each element, $P_{ei}(B,fe)$ is the joule loss of each element, B is the magnetic flux density and f_e is the frequency.

The efficiency is herein defined as

$$\eta = \frac{P_{out}}{P_{out} + P_{copper} + P_{iron}} \tag{6}$$

TABLE II
PERFORMANCE ESTIMATION FOR DSRFPMM AND DSAFPMM BY FEM

Item	Unit	Target	DSRFPMM	DSAFPMM
Cogging torque	Nm	-	1.826	1.135
Max. torque	Nm	207	208.8	208.8
Torque ripple	%	-	10.0	5.5
Max. output power	kW	60	60.5	60.5
Current density	A/mm^2	19	18	17
Efficiency@2768rpm	%	91	93.4	91.6
Max. power density	kW/L	10.2	10.24	10.24
Max. torque density	Nm/L	35	35.33	35.33
Magnet weight	kg	-	2.25	2.22
Core weight	kg	-	19.11	14.92
Power-weight ratio	kW/kg	-	2.5	2.8
Torque-weight ratio	Nm/kg	-	8.5	9.6

IV. CONCLUSION

In this paper, two traction motors with low cost ferrite magnets adopting the same novel structure have been proposed for HEVs. The two proposed motors named as DSRFPMM and DSAFPMM have been verified to have competitive performance such as torque/power density and efficiency with respect to a referenced rare earth magnet motor employed in a commercialized HEV (Toyota Prius) by FEM. It is also found that both proposed motors have good endurance against the irreversible demagnetization in ferrite magnets. Consequently, it is expected that both of the proposed ferrite magnet motors could be good alternatives for traction application replacing the need for rare earth magnets.

ACKNOWLEDGMENT

This research was supported by BK21PLUS program through the National Research Foundation of Korea funded by the Ministry of Education.

REFERENCES

[1] K. Kiyota and A. Chiba, "Design of Switched Reluctance Motor Competitive to 60-kW IPMSM in Third-Generation Hybrid Electric Vehicle," *IEEE Trans. on Ind. Appl*., vol. 48, no. 6, Nov. / Dec. 2012.

[2] T. Kosaka, T. Hirose and N. Matsui, "Experimental studies on drive performances of less rare-earth PM hybrid excitation motor," *in Proc. 2011 IEEE 8th Int. Conf. Power Electronics and ECCE Asia (ICPE & ECCE),* May 30–Jun. 3 2011, pp. 161–168.

[3] A. Chiba, Y. Takano, M. Takeno, T. Imakawa, N. Hoshi, M. Takemoto, and S. Ogasawara, "Torque density and efficiency improvements of a switched reluctance motor without rare-earth material for hybrid vehicles," *IEEE Trans. on Ind. Appl*., vol. 47, no. 3, pp.1240-1246, May/June 2011.

[4] S. Chino, S. Ogasawara, T. Miura, A. Chiba, M. Takemoto, and N. Hoshi, "Fundamental characteristics of a ferrite permanent magnet axial gap motor with segmented rotor structure for the hybrid electric vehicle," *in Proc. IEEE ECCE*, Sep. 17–22, 2011, pp. 2805–2811.

[5] T. Miura, S. Chino, M. Takemoto, S. Ogasawara, A. Chiba and N. Hoshi, "A ferrite permanent magnet axial gap motor with segmented rotor structure for the next generation hybrid vehicle," *in Proc. Int. Conf. Elect. Mach*., Rome, Italy, Sep. 2010, pp. 1–6.

[6] W.L. Zhao, T.A. Lipo and B.I. Kwon, "Design and Analysis of a Novel Dual Stator Axial Flux Spoke-type Ferrite Permanent Magnet Machine," *in Proc. 39th IEEE IECON*, Vienna, Austria, Nov. 2013, pp. 2714-2719.